CHANGES IN THE RAT ACL RESULTING FROM SUBFAILURE IMPINGEMENT LOADING

[1]David T. Fung, [2]J. Scott Quinby, [2]Jason L. Koh, [1]Shu Q. Liu and [1-3]Li-Qun Zhang
[1]Depts. of Biomed. Eng., [2]Ortho. Surg., and [3]Phy. Med. & Rehab., Northwestern University; email: d-fung@northwestern.edu

INTRODUCTION

While many noncontact ACL injuries may have resulted from direct over-stretching of the ligament, the ACL may also be injured due to its impingement against the intercondylar notch. Previous cadaveric studies have shown the ACL to impinge against the lateral wall of the notch during abduction and external tibial rotation at moderate knee flexion [1,2]. How impingement loading may alter the biomechanical properties of the ACL remains unknown. The purpose of this study was to evaluate changes in the force-length relationship of the ACL resulting from impingement, in corroboration with histological examinations on its superficial tissue, in a subfailure impingement injury model in rats

METHODS

Seven female musculoskeletally mature Sprague-Dawley rats with an average weight of 370±60 g (mean±SD) were used in this study. Under anesthesia, both lower limbs were disarticulated at the hip. Soft tissue on the disarticulated limbs was carefully dissected leaving only the ACL intact (Fig. 1a). The lateral tibial condyle of each femur-ACL-tibia complex (FATC) was then removed with a burring tool, allowing the knee to assume excessive abduction.

Each FATC was then mounted on a custom-designed loading apparatus with special clamps to hold the femoral and tibial shafts in a saline bath (Fig. 1b). In the apparatus, a linear motor with a precision of 0.4mm was used to load the ACL. A load cell was connected on one end to the motor shaft with its axis aligned with that of the load cell and, on the other end, to the tibial clamp. The FATC was secured into the apparatus by first fixing the tibia in the tibial clamp with the tibial axis aligned with the motor shaft and load cell axis. The femur was fixed to the femoral clamp, which, in turn, was attached to the multi-degree-of-freedom adjustable arm. Each FATC from each pair was randomly selected to be loaded in one of two knee postures by manipulating the position of the adjustable arm: 1) at ~30º flexion; and 2) at ~30º flexion, ~15º abduction, and ~5º external tibial rotation. Linear movement of the motor directly stretched the ACL longitudinally in the first posture and induced impingement of the ACL in the second.

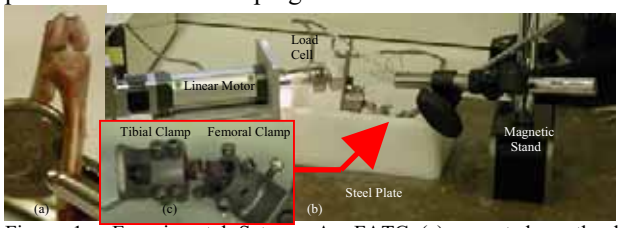

Figure 1. Experimental Setup. An FATC (a) mounted on the loading apparatus (b). Femoral and tibial clamps (c) secure the FATC, allowing the motor shaft the load the ACL cyclically.

Initially, the ACL was loaded cyclically to a minimal load to locate the 'inflection point' on the force-length curve, which established the ACL's normal length. The ACL was then preconditioned by loading the ACL 10× to 0.28 mm of displacement. Following preconditioning, the ACL was loaded repeatedly 10× at the same displacement (Sequence 1). The ligament was given a 15-min rest and loaded cyclically to 0.36 mm of displacement (Sequence 2) for 10 trials of 10 cycles per trial. Subfailure injury, if any, would have occurred during this Sequence, reaching 12% strain in the ligament. Following another 15-minute rest, the ligament was loaded cyclically 10× again at 0.28 mm of displacement (Sequence 3). All loading was applied at 1 mm/sec. Force-displacement data in Sequences 1 and 3 were plotted separately for impinged and nonimpinged ACL for each pair of FATC's. Using linear regression, the stiffnesses for the impinged ligament ($k_{1,imp}$ and $k_{3,imp}$) and for the directly-stretched ligament ($k_{1,ds}$ and $k_{3,ds}$) were determined in Sequences 1 and 3. Differences between the Sequences and between the mode of loading was evaluated statistically (Paired t-test). Significance was established at $p=0.05$.

Immediately following Sequence 3, the ACL was harvested and stained with a cell viability assay (Live/Dead® L-3224, Molecular Probes) with Hoechst 33258 added to locate the cell nuclei. Under the fluorescent microscope, live cells show green fluorescence and necrotic cells show red. Images were captured at 20× magnification and overlaid at randomly selected regions on impinged aspect, and the non-impinged aspect of the impinged ACL, and on the directly stretched ACL. The images of the three regions were compared to assess the effect of impingement.

RESULTS AND DISCUSSION

Among the seven pairs of ACLs, $k_{1,imp}$ (11.9±5.7 N/mm) (mean±SD) was significantly greater than $k_{3,imp}$ (9.6±6.0 N/mm) ($p=.014$). Insignificant difference was observed between $k_{1,ds}$ (12.9±7.1 N/mm) and $k_{3,ds}$ (12.1±5.5 N/mm) ($p=0.20$), and between $k_{1,ds}$ and $k_{1,imp}$ ($p=0.67$), demonstrating the impingement led to a reduction in the ligament's stiffness. Representative micrographs showed that impingement resulted in the disruption of the tissue organization and cell necrosis on the impinged surface of the ACL (Fig. 2).

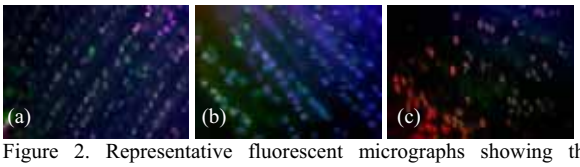

Figure 2. Representative fluorescent micrographs showing the directly stretched ACL (a), and the impinged ACL at its nonimpinged aspect (b) and impinged aspect (c).

CONCLUSIONS

Cyclic impingement loading has shown to decrease the stiffness of the ACL in the ex-vivo rat model, corroborated with reduced cell viability and disrupted tissue organization on the impinged surface of the ACL as observed on fluorescent micrographs. The loads and displacements reached during cyclic loading were within physiological limits. Results from this study contributed to our understanding of ACL injury resulting from impingement at the tissue level.

REFERENCES:

1.Fung, DT, Zhang, L-Q. (2003) *Clin. Biomech.* (18) 933-941.
2.LaPrade, RF, Burnett, QM. (1994) *AJSM*, (22) 198-203.